Three-Dimensional Finite Element Modeling of Pavements in Hawaii Considering Confinement Effect in Asphalt Surface Layers

FINAL PROJECT REPORT

By

Izak Said
University of Illinois at Urbana-Champaign
Michigan State University

Hasan Ozer
Arizona State University

Ricardo Archilla
University of Hawaii at Manoa

for

Center for Highway Pavement Preservation
(CHPP)

Disclaimer

The contents of this report reflect the authors' views — all of whom are responsible for the facts and accuracy of the data presented herein. The contents do not necessarily reflect the official views or policies of the Illinois Center for Transportation (ICT). This report does not constitute a standard, specification, or regulation. Trademark or manufacturers' names appear in this report as they are essential to the document's objective and do not constitute an endorsement of product by ICT.

<table>
<tr><td colspan="4">Technical Report Documentation Page</td></tr>
<tr><td>1. Report No.
CHPP Report-UIUC#8-2020</td><td>2. Government Accession No.</td><td colspan="2">3. Recipient's Catalog No.</td></tr>
<tr><td colspan="2" rowspan="2">4. Title and Subtitle
Three-Dimensional Finite Element Modeling of Pavements in Hawaii Considering Confinement Effect in Asphalt Surface Layers</td><td colspan="2">5. Report Date</td></tr>
<tr><td colspan="2">6. Performing Organization Code</td></tr>
<tr><td colspan="2">7. Author(s)
Izak Said, Hasan Ozer, Ricardo Archilla</td><td colspan="2">8. Performing Organization Report No.</td></tr>
<tr><td colspan="2" rowspan="2">9. Performing Organization Name and Address
Center for Highway Pavement Preservation,
Tier 1 University Transportation Center
Michigan State University, 2857 Jolly Road, Okemos, MI 48864</td><td colspan="2">10. Work Unit No. (TRAIS)</td></tr>
<tr><td colspan="2">11. Contract or Grant No.</td></tr>
<tr><td colspan="2" rowspan="2">12. Sponsoring Organization Name and Address</td><td colspan="2">13. Type of Report and Period Covered</td></tr>
<tr><td colspan="2">14. Sponsoring Agency Code</td></tr>
<tr><td colspan="4">15. Supplementary Notes</td></tr>
<tr><td colspan="4">16. Abstract
Asphalt concrete behavior is highly dependent on the temperature and frequency of loading. Traditionally, modulus of asphalt materials is characterized by performing creep recovery or complex modulus tests without considering the impact of lateral confinement level. Since the traffic-induced loading generates a multi-axial stress state within the pavement structure, quantifying the effect of lateral confinement on the global asphalt concrete behavior becomes a necessity. Previous studies have shown that dense-graded mixtures response is highly dependent on the confinement levels, especially at low frequencies and high temperatures. In this study, a constitutive model was developed for confinement-dependent linear viscoelastic behavior. The model was then incorporated into finite element pavement models using User-defined MATerial (UMAT). The numerical pavement models were used to quantify the impact of lateral confinement on pavement critical responses under various temperature profiles and tire loadings.
Accurate mechanistic models are essential especially for surface layers in environments like Hawaii. Capturing pavement responses accurately in the surface layers will contribute to the selection of surface preservation treatments such as thin overlays.</td></tr>
<tr><td colspan="2">17. Key Words</td><td colspan="2">18. Distribution Statement

No restrictions.</td></tr>
<tr><td>19. Security Classification (of this report)
Unclassified.</td><td>20. Security Classification (of this page)
Unclassified.</td><td>21. No. of Pages</td><td>22. Price

NA</td></tr>
</table>

Form DOT F 1700.7 (8-72) Reproduction of completed page authorized

List of Abbreviations

MEPDG: Mechanistic Empirical Design Guide
UMAT: User-defined MATerial

Acknowledgments

The authors would like to acknowledge the financial support of the Center for Highway Pavement Preservation.

Executive Summary

Asphalt concrete behavior is highly dependent on the temperature and frequency of loading. Traditionally, modulus of asphalt materials is characterized by performing creep recovery or complex modulus tests without considering the impact of lateral confinement level. Since the traffic-induced loading generates a multi-axial stress state within the pavement structure, quantifying the effect of lateral confinement on the global asphalt concrete behavior becomes a necessity. Previous studies have shown that dense-graded mixtures response is highly dependent on the confinement levels, especially at low frequencies and high temperatures. In this study, a constitutive model was developed for confinement-dependent linear viscoelastic behavior. The model was then incorporated into finite element pavement models using User-defined MATerial (UMAT). The numerical pavement models were used to quantify the impact of lateral confinement on pavement critical responses under various temperature profiles and tire loadings.

Accurate mechanistic models are essential especially for surface layers in environments like that of Hawaii. Capturing pavement responses accurately in the surface layers will contribute to the selection of surface preservation treatments such as thin overlays.

CHAPTER 1. INTRODUCTION

1.1 MOTIVATION AND BACKGROUND

Traditionally, asphalt concrete (AC) modulus has been determined experimentally unconfined and incorporated into the structural analysis for thickness design and performance prediction. However, for dense graded mixtures, it has been shown that the effect of confinement can substantially affect the AC modulus (Corrales-Azofeifa and Archilla 2018).

There is a concern that the design and analysis conducted without confinement in the AC layers is not capable of capturing complex stress states in the surface AC layers resulting in inaccurate distress predictions. In the previous CHPP study, it was shown that stress states are complex within the thin overlays (Al-Qadi et al., 2018). More accurate constitutive models for asphalt mixes to represent such stress states can be important to improve accuracy of performance predictions.

The earlier work by Archilla (2015) to model pavement structures in Hawaii included a linear elastic static analysis performed with an axisymmetric finite element program. The following assumptions were made: 1) it simulated a limited domain of 200 in. in depth by 200 in. in radius, 2) the load was assumed to be circular with 5.91 in. radius (as applied by an FWD) and with constant pressure, 3) the load was static instead of dynamic and rolling, 4) no viscoelastic effects were considered, and 5) the frequency determination in the MEPDG was used.

The linear viscoelasticity implementation in a 3-D finite element model can be used to address some of the complexities of pavement deformations. Linear viscoelasticity is accepted as the main constitutive relationship used in mechanistic analysis of pavements (Monismith and Secor; 1962; Goodrich, 1988; Park et al, 1996; Elseifi et al, 2006). Even though a one to one relationship between linear viscoelastic representation of pavements and distresses do not exist, 3-D FE models with linear viscoelastic asphalt layers can be used to realistically predict complex stress states and strains.

However, the effect of confinement can be an additional factor amplifying the complexity of near surface deformations. Considering the fact that many of the preservation treatments are thin layer applications on a pavement surface, the importance of capturing near surface pavement responses can be recognized. It can be hypothesized that the distresses initiated or concentrated on the surface will be affected by confinement more severely. Consideration of confinement near the surface under complex three-dimensional contact stresses may especially affect rutting and top-down cracking type of distresses and other failure mechanisms in preservation treatments. Therefore, there is a need for three-dimensional structural analysis of typical pavement sections with consideration of confinement in the AC layers.

1.2 OBJECTIVES

The purpose of this research is to provide a fundamental understanding of the mechanics of the rutting and top-down cracking problem to include the effect of confinement level using three-dimensional modeling approach. The expertise of the University of Illinois at Urbana-Champaign's research team on the finite element modeling was leveraged. Some of the key features of the three-dimensional finite element model included dynamic analysis, moving load, linear viscoelastic properties of AC layers, interaction between layers, and 3-D and non-uniform contact stresses.

1.3 METHODOLOGY

The finite element modeling approach was used in the study. In addition to the standard features developed earlier by Al-Qadi and his colleagues (Al-Qadi et al., 2005; Yoo et al., 2006; Al-Qadi and Yoo, 2007; Yoo and Al-Qadi, 2007), a user-material (UMAT) subroutine was developed to model confinement effect while considering linear viscoelasticity for asphalt materials. A thick AC pavement section representative was chosen for modeling. Field measured temperature profiles were used along with experimental data for an AC mix commonly used in Hawaii. Three load cases were completed at five temperature profiles occurring during the day with two hours intervals. The results from the finite element models were analyzed to evaluate the impact of confinement on predictor stresses and strains indicative of rutting and top-down cracking.

1.4 REPORT CONTENT AND ORGANIZATION

The University of Illinois at Urbana-Champaign (UIUC) and University of Hawaii at Manoa (UHM) research teams collaborated in this project. The final report is organized as follows:

- Chapter 1 Introduction
- Chapter 2 Research Approach
- Chapter 3 Modeling Cases and Analysis of Results
- Chapter 4 Conclusions

CHAPTER 2. RESEARCH APPROACH

2.1 EXPERIMENTAL EFFECT OF CONFINEMENT

Temperature Gradients

Temperature profiles at different times of the day (10:00, 12:00, 14:00, 16:00, and 18:00) were determined and shown in Figure 2.1. The data used were computed using a finite difference model developed by Archilla (2015). The model was developed based on the one-dimensional diffusion law that governs the vertical heat flow in the pavement structure. The finite difference procedure was the numerical technique used to solve the second order differential equation. The results were validated using an experimental setting (Archilla 2020). The setting consisted of a pavement core (300 mm Hot Mix Asphalt [HMA] and 150 mm granular material) insulated horizontally using styrofoam to allow unidirectional heat flow (vertical). Thermocouples were placed at various depths within the HMA layer (0.25, 0.75, 1.5, 2.5, 3.5, 6, 10, and 12 in). The depths selected correspond to the mid-points of the sublayers in the sublayering recommended for modeling the pavement responses for a 300 mm HMA layer thickness in the pavement mechanistic-empirical design guide (MEPDG). The specimen was placed in the field and the data were collected using a data logger. Results showed a good match between measured, and predicted temperatures, especially within the first 150 mm).

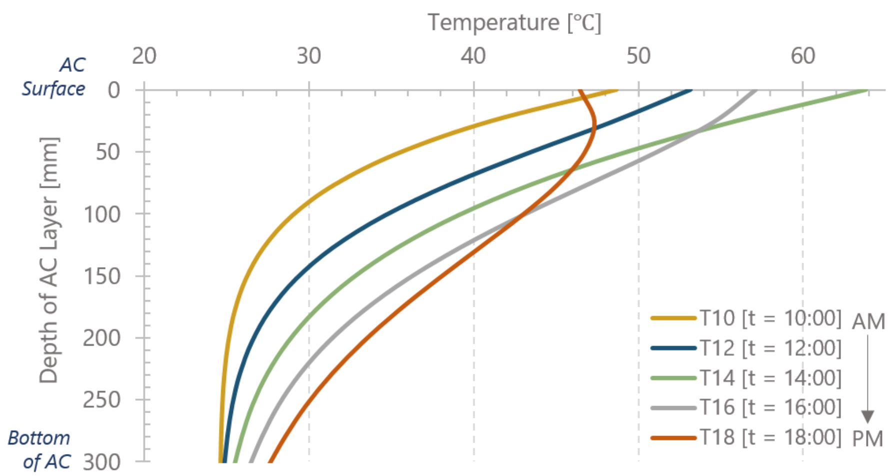

Figure 2-1. Temperature profiles with the AC layer at different times within the day

Complex Modulus Characterization

Typical tests to obtain linear viscoelastic relaxation modulus or creep compliance involve stress relaxation and creep tests, respectively. In a stress relaxation, a constant strain is applied to the specimen and stress is measured as it relaxes with time. On the other hand, creep tests include constant stress application and measurement of increasing strain with time. In addition to these tests, frequency-dependent loading is commonly used to find complex modulus of the viscoelastic materials. The outcome of this test is the frequency-dependent modulus of the material. It is also important to note that modulus is measured as a function of frequency of loading and needs to be converted to real time domain by conversion techniques.

All of these aforementioned tests are conducted at different temperatures to characterize the temperature-time dependent behavior of the material. An important property for some of the viscoelastic materials valid at certain conditions is utilized to incorporate temperature and time dependency of the viscoelastic materials. This property is called time-temperature superposition and it is valid only for thermo-rheological simple materials and can be limited to a certain temperature range. An example of time-temperature superposition rule is shown during the construction of master modulus curves. The modulus is determined experimentally at different temperatures and the data at each temperature is then shifted horizontally to form a single master curve at a reference temperature. Each modulus master curve shows how complex modulus increases with frequency of loading. At a very high frequency, material will have no time to damp strains; therefore, behaves like an elastic material.

In this study, the asphalt mixture tested is composed of PG64-16 binder and 4% air void. The remaining mixture characteristics are summarized in Table 2.1. The dynamic modulus test was performed with lateral confinements ranging from 0 to 1000 kPa. The test was conducted for each confinement level under different temperatures (4, 20, 40°C) and frequencies (0.1, 1, 5, 10, 25 Hz) combinations. Four replicates were tested for each temperature/frequency combination. The resulting modulus data were then used to develop the AC master curves for the various confinement levels considered (Figure 2.2).

Table 2-1. Mixture characteristics

Percent Binder [% by Mass]	6.1
Absorbed Binder [% by Mass]	1.46
Effective Binder [% By Mass]	4.73
Actual Air Void [%]	3.53
Voids in Mineral Aggregate [%]	14.5

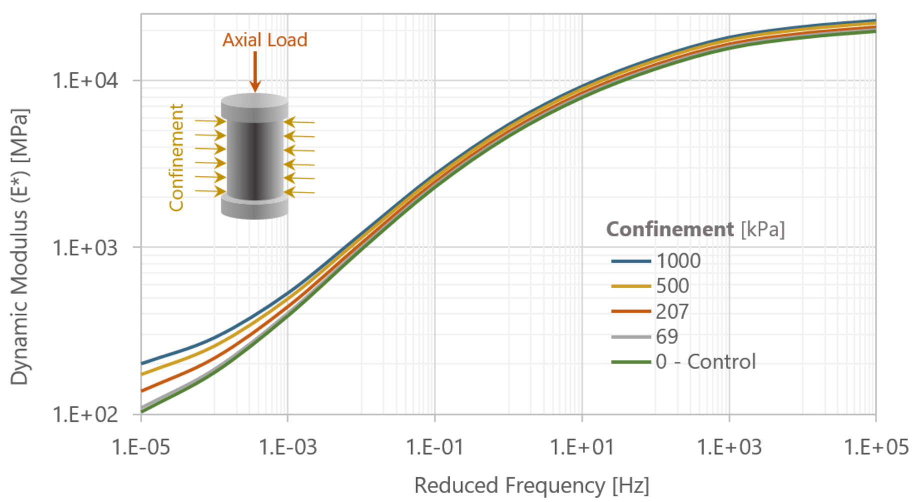

Figure 2-2. Master curve of AC mixture at various lateral confinement levels

Confinement Model

A predictive model was developed for viscoelastic master curves as a function of the confinement level. The model form is presented in equation 2.

$$\textbf{LVE} \qquad E(t) = E_0 - \sum_{n=1}^{N} E_i\,(1 - \exp(-t/\tau_n)) \tag{1}$$

$$\textbf{CDV} \qquad E(t) = g_0 E_0 - \sum_{n=1}^{N} g_1 E_i\,(1 - \exp(-t/\tau_n)) \tag{2}$$

where: E (t) = relaxation modulus at time t; E_0= instantaneous relaxation modulus; N = number of dashpot-spring; E_i = spring constant; τ_n = relaxation time. g_0 and g_1 are non-linear parameters that describe the impact of confinement level on the instantaneous relaxation modulus and spring coefficients, respectively. The fitted equations for these parameters are presented in equation 3-4.

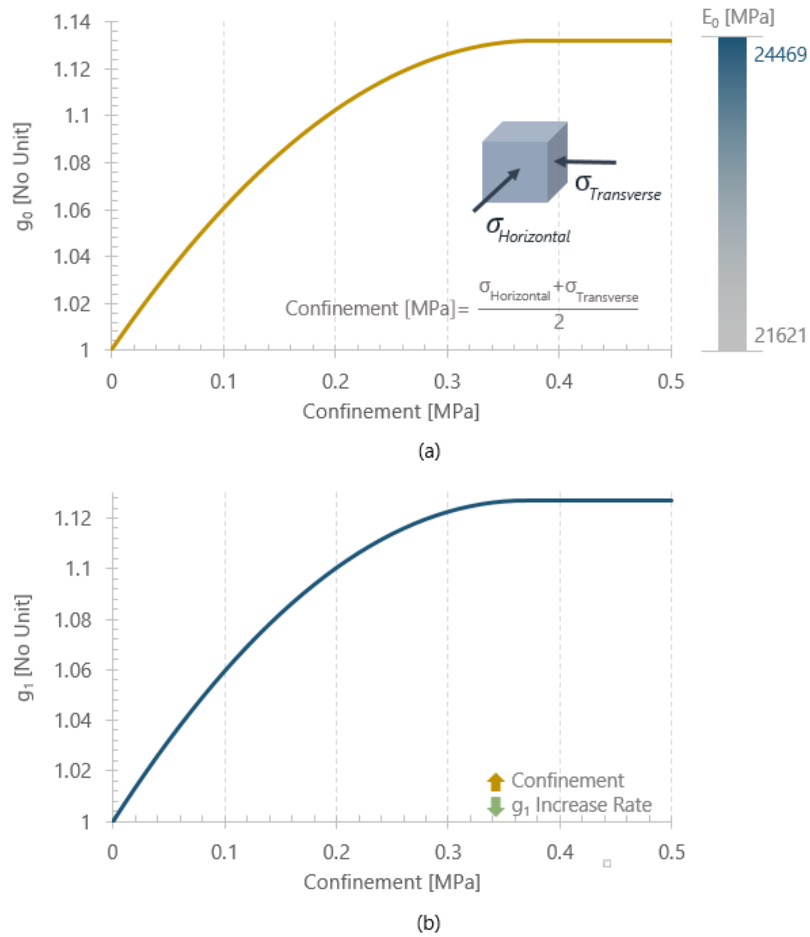

Figure 2-3. The value of g0 and g1 in function of confinement level

$$g_0 = 1.19 \times (\sigma_c + 0.1)^{0.071} \tag{3}$$

$$g_1 = 1.195 \times (\sigma_c + 0.1)^{0.074} \tag{4}$$

2.2 FINITE ELEMENT MODEL

Finite element modeling (FEM) is used in this study to compute the critical pavement responses. The numerical model includes variables usually omitted from conventional pavement design and analysis, such as dynamic-implicit analysis, continuous moving load with appropriate load amplitude variation, three-dimensional contact stresses, linear viscoelastic, and confinement dependent asphalt concrete behavior, use of infinite elements, and a Coulomb model to represent the layer interface. Previous studies have showed the importance of considering these factors for accurate prediction of pavement critical responses. The numerical matrix considers two asphalt material models (linear viscoelastic and confinement-dependent viscoelastic), three load levels ranging from low to high, and five temperature profiles (Figure 2.4). These profiles represent the fluctuations in asphalt concrete temperature distribution within the day. The linear viscoelastic cases are used as reference cases; they allow the quantification of the impact of lateral confinement. The load and temperature factors were considered because they are expected to highly influence the pavement responses when the effect of confinement is considered. The speed was selected to be relatively low (8km/h) to simulate a critical condition for a linear viscoelastic material. Low-frequency load applications cause the AC modulus to decrease, consequently increasing pavement responses.

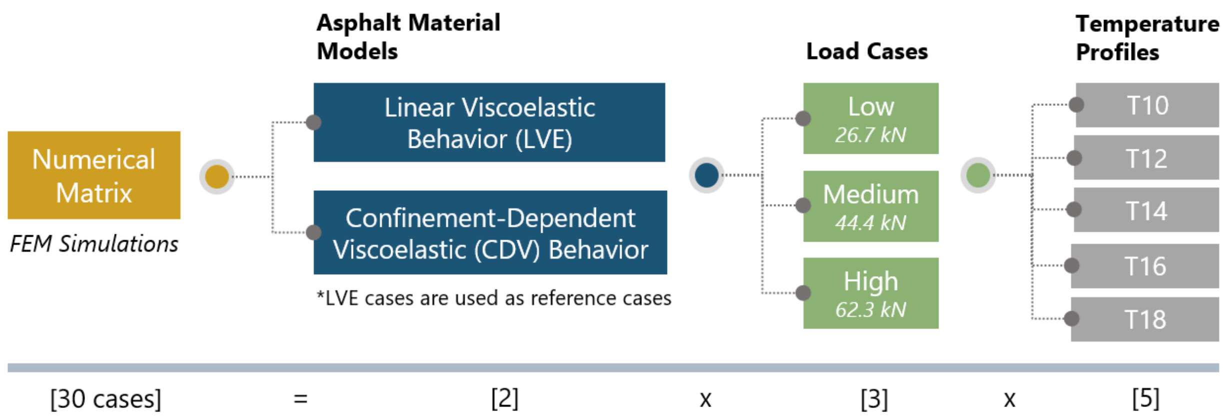

Figure 2-4. Finite element numerical matrix

The pavement structure consists of three layers: A semi-infinite subgrade layer, a 300 mm base layer, and a 300 mm asphalt concrete layer. The pavement configuration, material models, and layers interaction used are presented in Figure 2.5.

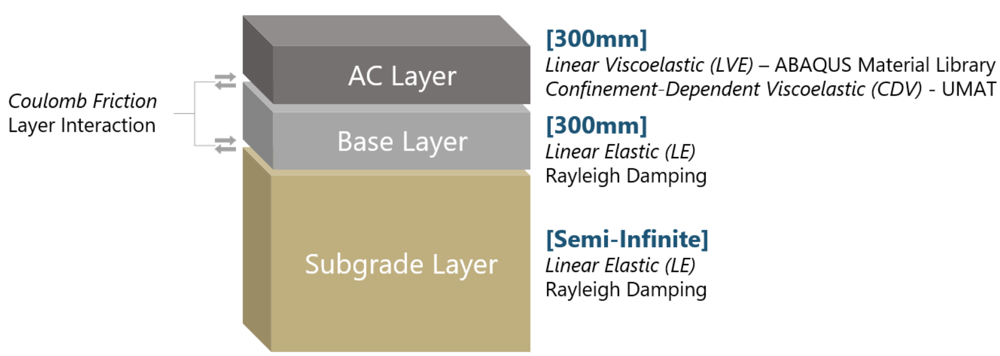

Figure 2-5. Pavement configuration and material models

The asphalt concrete layer was modeled as a linear viscoelastic and confinement-dependent linear viscoelastic material. The viscoelastic material model in Abaqus was used when confinement is not considered. For these cases, the material characteristics used were based on the dynamic modulus test results at a zero-confinement level. For the numerical simulations that include the effect of confinement, the UMAT developed in this study was used as a replacement to the viscoelastic material model available in the Abaqus material library. The soil's behavior is stress-dependent, but since the asphalt concrete thickness is relatively high, it is assumed that the stress dependency effect is negligible. Therefore, the base and subgrade layers were modeled as linear elastic materials. Typical resilient modulus, Poisson's ratio, and Rayleigh damping parameters were selected for this study. All material properties used are reported in Table 2.2. The layer interface is numerically simulated using the Coulomb friction model with a shear stress limit of 1.415 MPa at the AC-Base interface and 0 MPa at the Base-Subgrade contact.

Table 2-2. Material Properties

Instantaneous Properties

E_0 [MPa]	ν
21621.24	0.30

Prony Parameters

τ_i [s]	E_i [MPa]
0.00001	3010.28
0.0001	329.85
0.001	3675.20
0.01	3981.92
0.1	3824.06
1	3118.78
10	2037.82
100	1002.60
1000	376.64
10000	127.85
100000	52.11

Williams–Landel–Ferry (WLF) parameters are reference temperature 20°C, C_1 = 22.1, C_2 = 167.48

(a)

Base Elastic Properties

M_R [MPa]	ν
206.8	0.35

Subgrade Elastic Properties

M_R [MPa]	ν
82.7	0.40

For base and subgrade, the Rayleigh damping parameters are α = 3.1416 and β = 0.000795

(b)

A mesh sensitivity analysis was performed to optimize the accuracy of the finite element model responses and computational cost. The finite element models are divided into three main zones. (1) The wheel path; the area where the load is dynamically applied. The finest mesh is used in the area (~10 x 20 mm) since it is the location where critical pavement responses are collected. (2) Transition zone; a gradual change in element size in this area allows a reduction in computational cost. Element size increase toward the outer edges of the pavement model (up to 300 x 300 mm on the corners). (3) Infinite elements; reduce the use of artificial boundary conditions. The model dimensions are presented in Figure 2.6. Eight-node brick elements (C3D8 in Abaqus) are used in the AC and base layer (2x2x2 integration points/elements). To reduce computational time, C3D8 with reduced integration points were used in the subgrade (C3D8R, one integration point/element). Three-dimensional solid continuum infinite elements of type CIN3D8 were used on the model boundaries (8-node linear, one-way infinite).

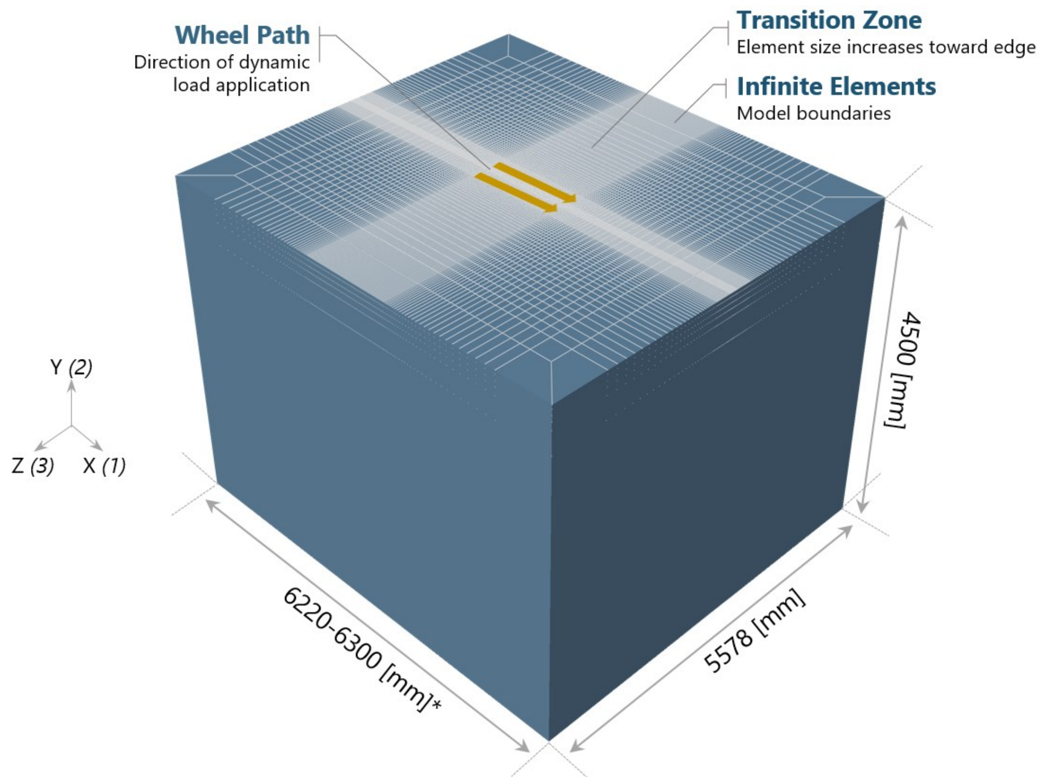

Figure 2-6. Pavement numerical model with dimensions

Conventional pavement analysis assumes static loading, uniform vertical contact pressure, circular or rectangular tire-pavement contact. These assumptions do not accurately represent the contact area and load distribution at the tire-road interface, which is three dimensional with nonuniform magnitude. The use of three-dimensional contact stresses is crucial for the prediction of accurate near-surface pavement responses and resultant damage, especially near the surface. In this study, experimental measurements of three-dimensional contact stresses were used. Figure 2.7 shows the vertical, transverse, and longitudinal load distribution. This study's three-dimensional contact forces are based on measured data collected using the dual SIM Mk IV system deployed in South Africa. This system consists of two pads instrumented with steel pins that measure the contact forces in the vertical, transverse, and longitudinal directions. The tire used in a DTA 275/80R22.5 with an inflation pressure of 690 kPa loaded at 26.7, 44.4, and 62.3 kN.

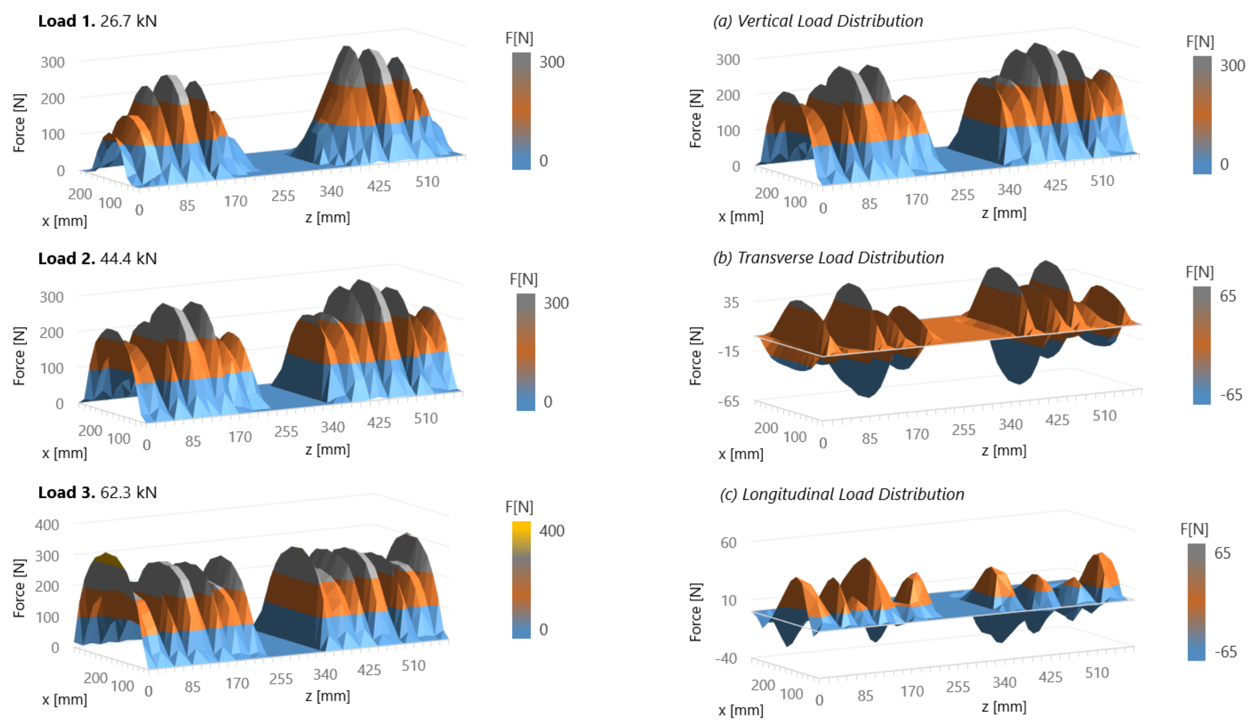

Figure 2-7. Three-dimensional load distribution

2.2 DEVELOPMENT OF UMAT

The effect of confinement was integrated to a linear viscoelastic material model using a user material subroutine (UMAT). The UMAT was developed on top of a linear viscoelastic material constitutive relationship. The hereditary integral formulation for stress-strain relationship for a viscoelastic material is expressed as follows. This equation was modified to incorporate the effect of confinement.

For an isotropic material, this relationship can reduce to:

$$\sigma_{ij}(t) = \int_0^t 2G(\xi - \xi')\frac{de_{ij}}{d\xi'}d\xi' + \delta_{ij}\int_0^t K(\xi - \xi')\frac{d\varepsilon_v}{d\xi'}d\xi' \qquad (4)$$

where total strain is expressed with deviatoric (S_{ij} and e_{ij})and volumetric components (P_{ij} and ε_v). $\sigma_{ij} = S_{ij} + P_{ij}$; $\varepsilon_{ij} = e_{ij} + \frac{1}{3}\delta_{ij}\varepsilon_{kk}$; $\varepsilon_v = \varepsilon_{kk}$; $P_{ij} = \delta_{ij}p = -\frac{1}{3}\delta_{ij}\sigma_{kk}$. Table 2-3 presents the flow of the algorithm implemented in Abaqus.

The linear viscoelasticity algorithm requires calculation of the tangent stiffness as an estimate of the stiffness at a given displacement for a linear system. Once the effect of confinement is added to the constitutive stress and strain relationship, the system is no longer linear. Therefore, tangent stiffness calculated using Equation (5) is just an estimate of the stiffness and can cause slow convergence of the system of equations. A summary of the implementation of the CDV is given with the flowchart below.

$$C_{ijkl}^{n+1} = G_T^{n+1}[I_{ijkl} - \frac{1}{3}\delta_{ij}\delta_{kl}] + K_T^{n+1}\delta_{ij}\delta_{kl} \tag{5}$$

Table 2-3. Pseudo-code developed for confinement effect

Steps. User-Defined Material model (UMAT) for *Confinement-Dependent Viscoelastic (CDV)* materials		**Variables**
1	UMAT get the stress state and state variables from the previously converged time step t_n	ξ_n, σ_{ij}^n, STATEV
2	Calculate instantaneous modulus and Prony coefficients based on the confinement level of the previous converged time step t_n	E_0, E_i
3	Calculate increment time and reduce time	t_{n+1}, ξ_{n+1}
4	Compute total deviatoric and volumetric strain increment	$\Delta e_{ij}^{n+1}, \Delta\varepsilon_v^{n+1}$
5	Calculate pseudo strain increment for each component of Prony series	$\Delta e_{kl}^m, \Delta\varepsilon_v^m$
6	Calculate deviatoric and volumetric stress increment	$\Delta S_{kl}^{n+1}, \Delta p^{n+1}$
7	Calculate tangent stiffness and update stress tensor	$G_T^{n+1}, K_T^{n+1}, C_{ijkl}^{n+1}$
8	Return stress tensor and state variables to the main program	σ_{ij}^{n+1}, STATEV

CHAPTER 3. RESULTS AND DISCUSSION

3.1 EFFECTS OF CONFINEMENT ON STRESS AND STRAIN STATES

Figure 3.1 shows the confinement distribution within the asphalt concrete layer at various load levels (26.7, 44.4, and 62.3 kN) and temperatures (T10 and T14). The confinement is calculated by averaging the longitudinal and transverse normal stresses. A positive and negative confinement value indicates a compressive and tensile stress state, respectively. While high compressive confinement means areas of high modulus, tensile confinement is assumed not to have any impacts on the material mechanical properties. Thus, the responses at the bottom of the AC layer from both AC material models considered are expected to be close. The highest compressive confinement is found directly underneath the tire near the tire treads.

The confinement level increases with increasing temperature. Asphalt concrete has viscoelastic behavior. Therefore, its response to load excitations is time-, temperature-, and load history-dependent. Asphalt concrete becomes more viscous at high temperatures, leading to a decrease in modulus and, consequently, higher responses and confinement values. In addition to increasing confinement, the increase in temperature causes the depth of compressive confinement to increase. As expected, the increase in loading causes higher confinement level and deeper zones of influence.

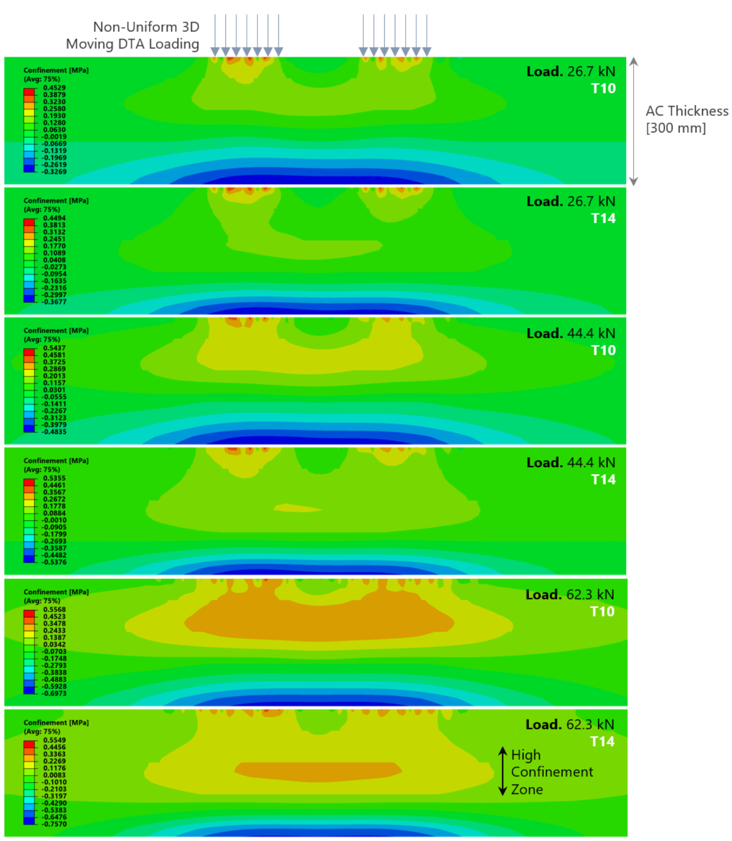

Figure 3-1. Confinement distribution within the AC layers

Figure 3.2 displays the vertical strain at an element 10 millimeters below the AC surface. For the selected element, the vertical strain time history was collected for extreme load and temperature values. Figure 3.2 (top) shows the vertical strain time history for a truck tire load of 26.7 kN; Figure 3.2 (bottom) shows the same response for a higher load of 62.3 kN. Temperatures T10 and T14 represent the highest and lowest AC temperature profiles, respectively. The x-axis maximum value (0.486 seconds) represents the time needed for a truck to drive 1.22 meters at a speed of 5 mph. Between 0 and 0.19 seconds, the vertical strain is zero, indicating the approaching truck tire did not affect the responses at the location of interest. Between 0.19 seconds 0.23 seconds, the element was under horizontal tensile stresses. Therefore, the confinement did not affect modulus, and consequently, the responses from LVE and CDVE were identical. Following the first 0.23 seconds, the element was under compressive confinement, which caused the material modulus to increase, resulting in lower vertical strain. The difference in the vertical strain from the LVE and CDVE models increased with increasing temperature. The effect of confinement was also noticeable during the recovery of the AC material (unloading). Note that the effect of confinement on the vertical strain during loading and unloading was similar for the two loadings considered (26.7 and 62.3kN).

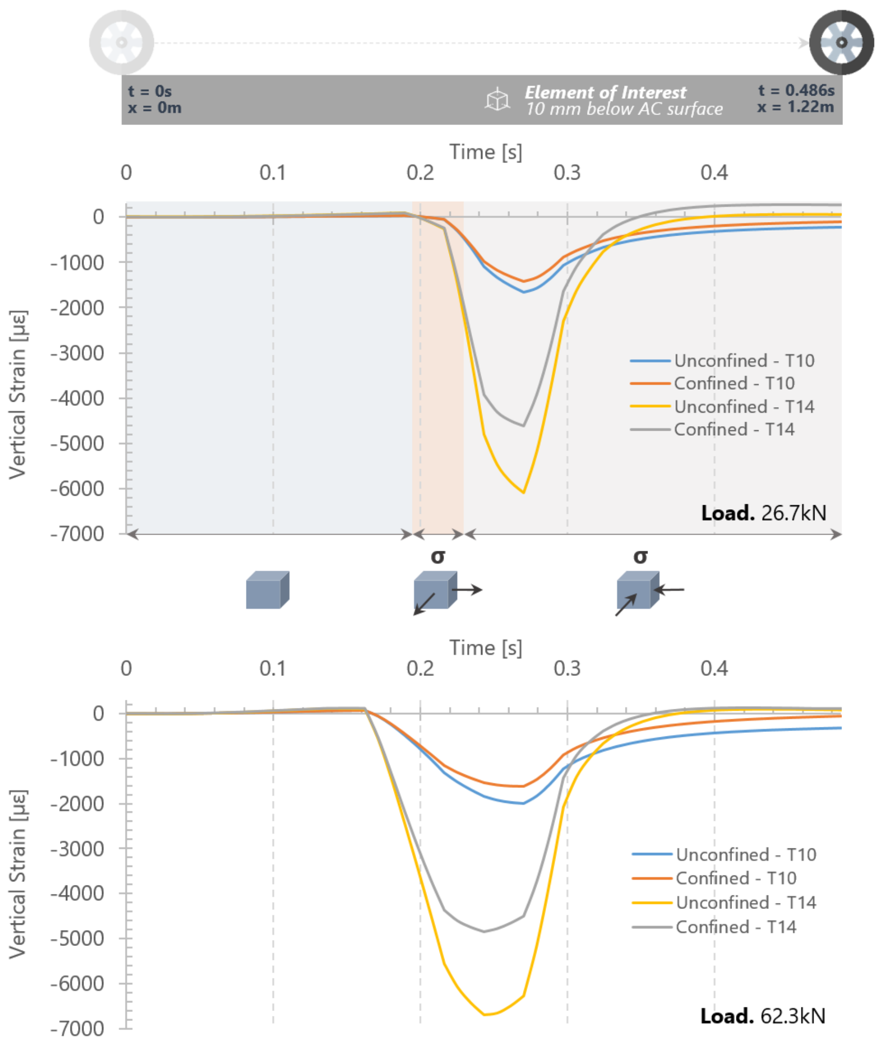

Figure 3-2. Vertical strain along the path 10 mm below the AC surface

Figure 3.3 shows the vertical strain difference between LVE and CDVE models along path A-B, which is 10 millimeters below the AC surface. The maximum compressive vertical strain is expected to be at the tire-pavement interface. The path was selected to be 10 mm below the AC surface to reduce the effect of boundary condition, which might be affected by how the load is applied to the pavement model. The shown difference in vertical strain was computed by subtracting the vertical strain of the CDVE from the same response in the LVE models. The x-axis encompasses the width of the two tires (2x222 mm), the spacing between the tire (136 mm), and around 100 mm on the external edges of the tires. By examining the results, it can be noticed that the maximum difference in vertical strain value is mostly affected by the temperature. While the increase in loads had a lower impact on the vertical strain difference than temperature, this increase caused a higher vertical stress/strain area under the tire. The difference in vertical strain between the tires was negligible. The elements in this location are under tension, which resulted in no effect of confinement and, consequently, unchanged material properties.

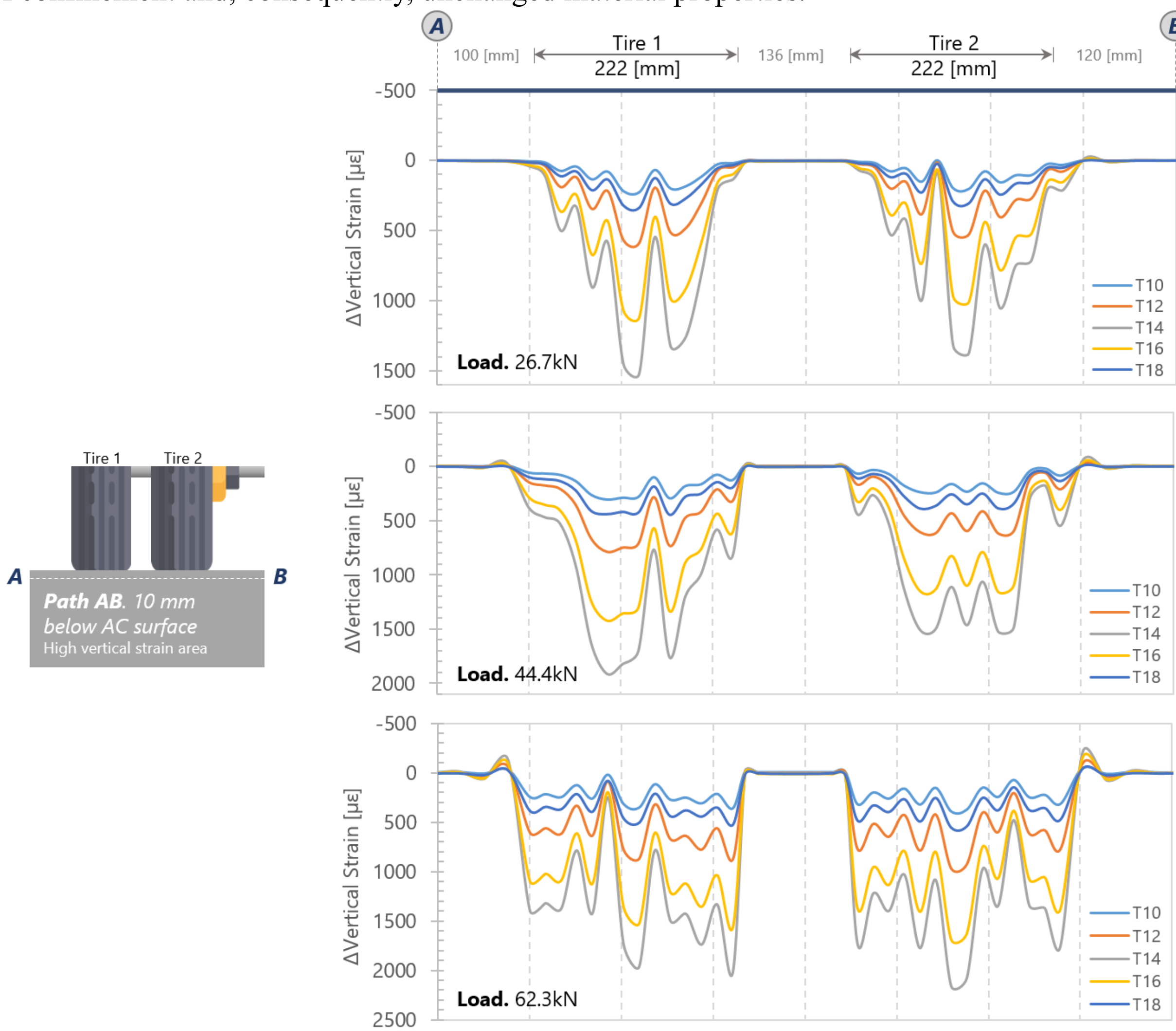

Figure 3-3. Vertical strain along the path 10 mm below the AC surface

Figure 3.4 displays the impact of the confinement on the vertical strain along (1) vertical pass underneath the center of the tire (EF) and (2) vertical path at the edge of the tire (CD). The difference in vertical strain along the vertical path indicated the impact of confinement on the reduction of rutting within the AC layer. A higher difference in vertical strain was observed at higher temperatures. Moreover, the highest vertical strain was found at the surface of the AC. Figure 3.4 shows that the impact of confinement on the vertical strain is limited to the first 150 mm from the AC surface. Below this depth, the effect of confinement becomes negligible because the lower 150 mm is under tensile stress/strain state. The difference in vertical strain increased significantly with the increase in loading. Finally, in general, a higher reduction in the vertical strain between LVE and CDVE models is underneath the center of the tire as compared to the path located at the edge of the tire.

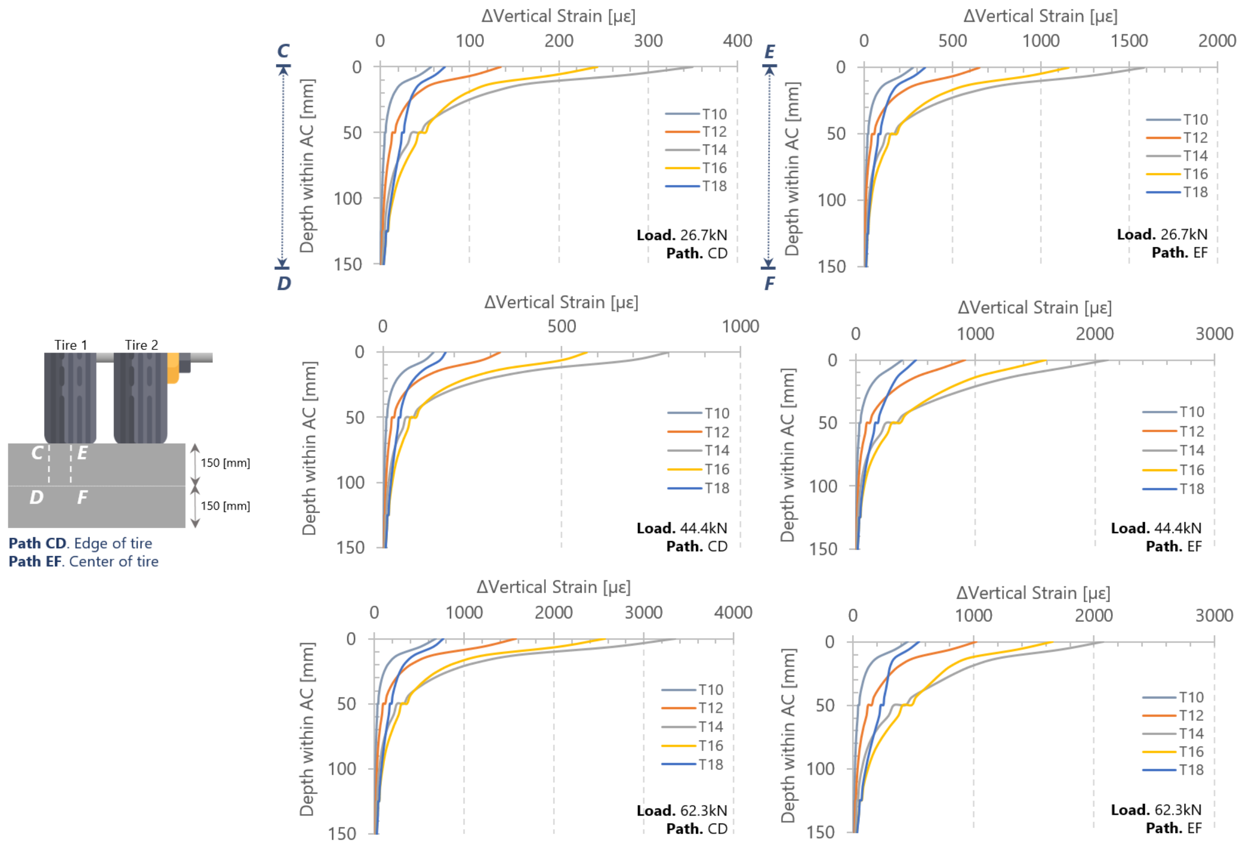

Figure 3-4. Vertical strain along vertical paths under the center and at the edge of tire are various load values and temperature profiles.

Figure 3.5 presents the shear strain at an element 50 millimeters below the AC surface versus time. The maximum shear strain within the AC layer is usually reported at a depth of 50 mm within the AC layer. The shear strains were collected and plotted for the minimum and maximum loads and temperature profiles considered. Initially, the shear strain from LVE and CDVE models are similar because the element of interest is under tension. When the element becomes in compression, the impact of confinement becomes significant. At low temperatures, the effect of confinement is almost negligible. At high temperature and/or load, a substantial reduction in shear strain was observed in the CDVE model. Both maximum shear value and the recovery of the AC material were affected; confinement allowed the AC material recovers faster.

The difference in shear strain along path GH at various loads and temperatures is plotted in Figure 3.6. Unlike the difference in vertical strain, the vertical shear reduction due to confinement is profoundly affected by the applied load values. The shear strain reduction increased from 90 to 335με with the increase in load from 26.7 to 62.3 kN. Even though the highest shear strain was found at T14, the highest response reduction along GH was with the T16 temperature profile. The impact of confinement was more pronounced at the edges of the tires as compared to the area underneath the tire.

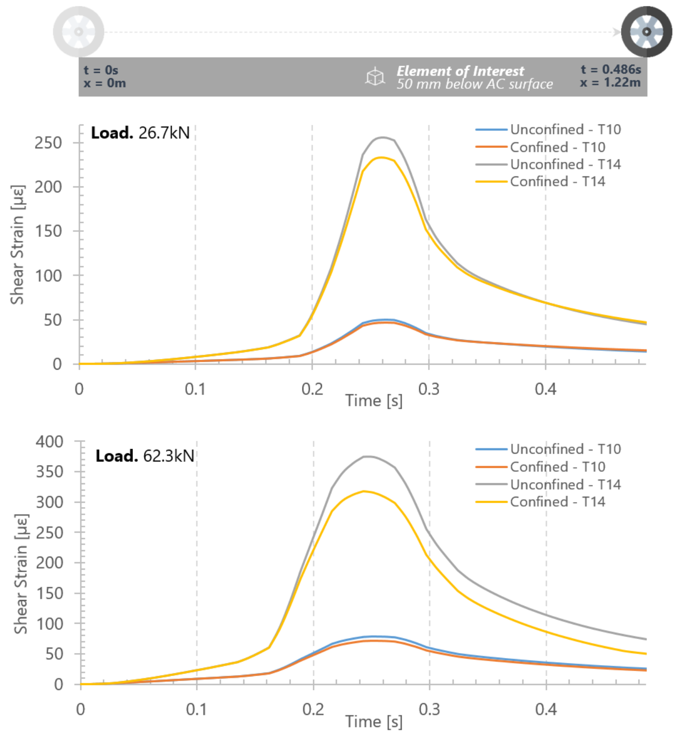

Figure 3-5. Shear strain time history at an element 50 mm below the AC surface

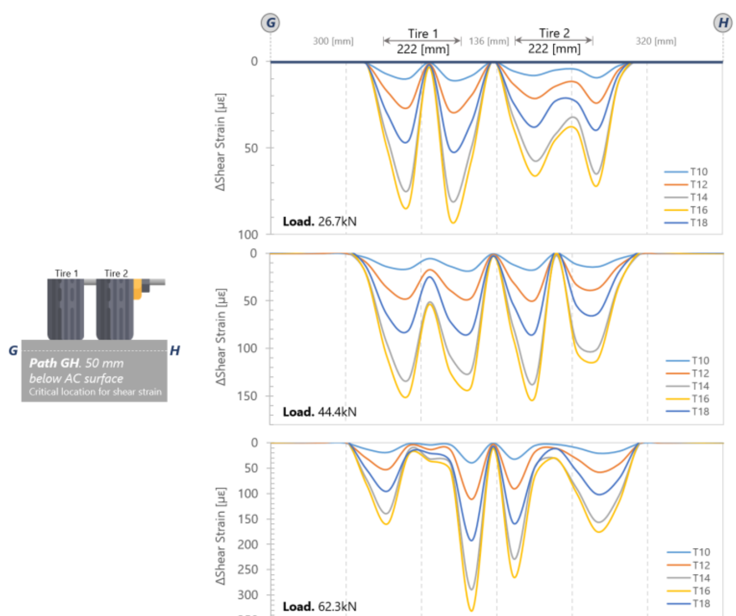

Figure 3-6. Shear strain along the path 50 mm below the AC surface at various load values and temperature profiles

The effect of confinement on shear strain along vertical paths near (KL) and at the edge of the tire

(IJ) was investigated (Figure 3.7). At the side of the tire, in general, the highest difference in shear strain was found to be at 50 mm. On the other hand, the highest impact of confinement was found to be close to the area directly under the tire loading. This is mainly caused by the high compression and confinement under the tire-pavement contact area.

The percentage reduction on the vertical and shear strain within the AC layer are summarized in Figures 3.8-a and 3.8-b, respectively. The maximum percent decrease in vertical strain and shear strain due to the incorporation of the CDVE model was found to be 31% and 17.5% for the highest load-temperature combination. Moreover, the impact of confinement generally increased with increasing temperature and increasing load.

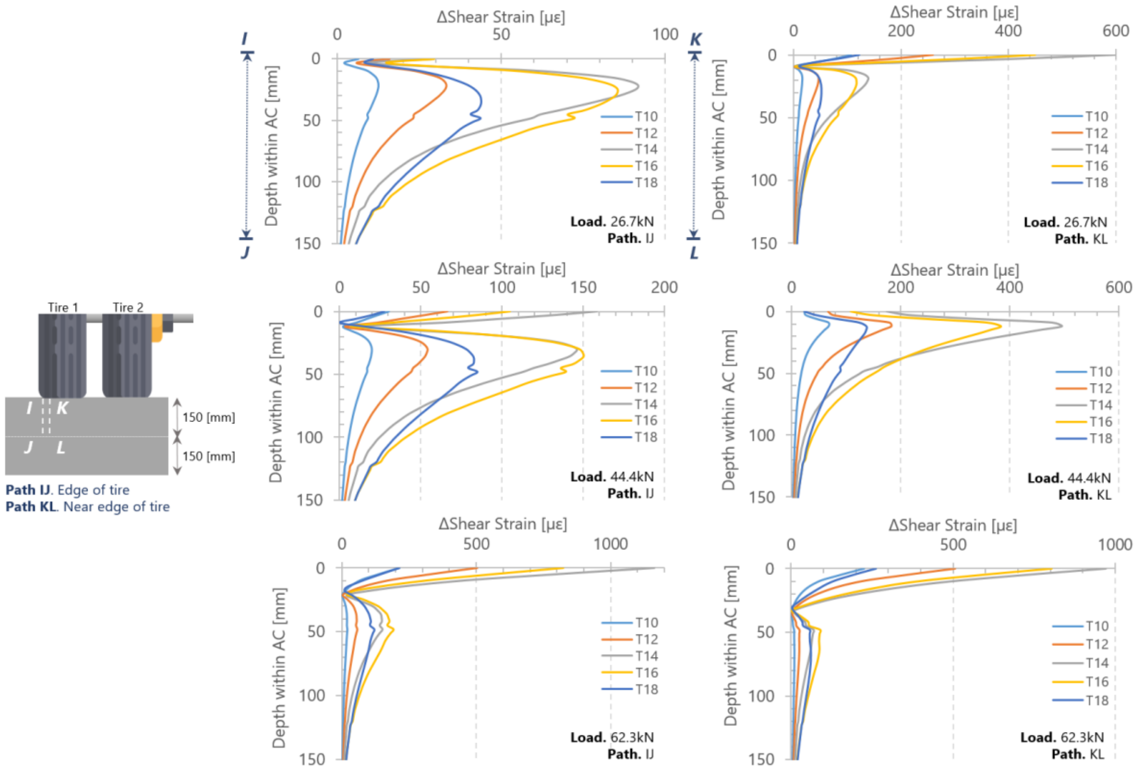

Figure 3-7. Shear strain along vertical paths near and at the edge of tire

3.2 NEAR SURFACE MAXIMUM PRINCIPAL TENSILE STRAINS

The near-surface tensile maximum principle strain can also be used to describe mechanisms of top-down cracking. This response is usually limited to the first 50 mm within the AC layer, as shown in Figure 3.9. Table 3.1 summarizes the maximum tensile principal strains for the various temperature profiles, material models, and loading values considered. As expected, the strain value increased with increasing temperature and/or loading. The percentages difference (decreases) in maximum principal tensile strain between LVE and CDVE models for all load-temperature combinations are presented in Figure 3.10.

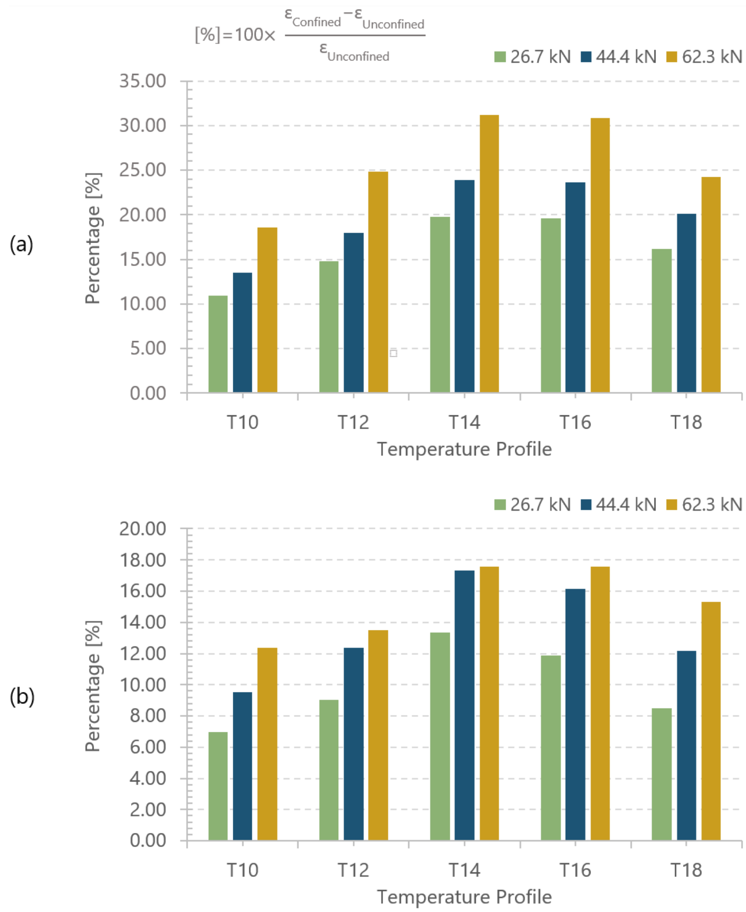

Figure 3-8. Percentage decrease in (a) vertical strain and (b) shear strain caused by the incorporation on confinement effect on AC modulus.

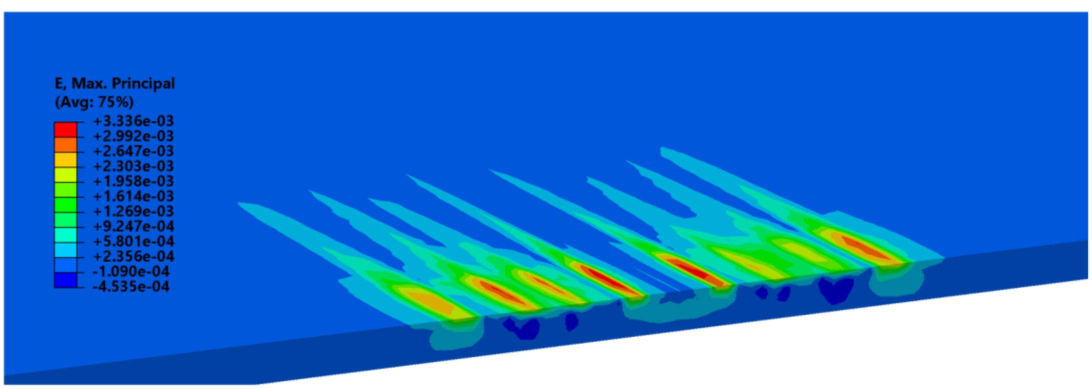

Figure 3-9. Maximum principal strain distribution within the top 50 mm of the AC layer.

Table 3-1. Maximum tensile principal strain for the various loads, temperature profiles and material models considered.

		Load [kN]		
Temp.	Model	26.7	44.4	62.3
T10	LVE	628.7	805.2	1135
	CDVE	560.2	712.5	1039
T12	LVE	1118	1495	1967
	CDVE	970.5	1275	1732
T14	LVE	2069	2683	3572
	CDVE	1790	2215	2828
T16	LVE	1619	2011	2800
	CDVE	1352	1637	2329
T18	LVE	693.6	888	1282
	CDVE	619.2	799	1133

*Responses are in με

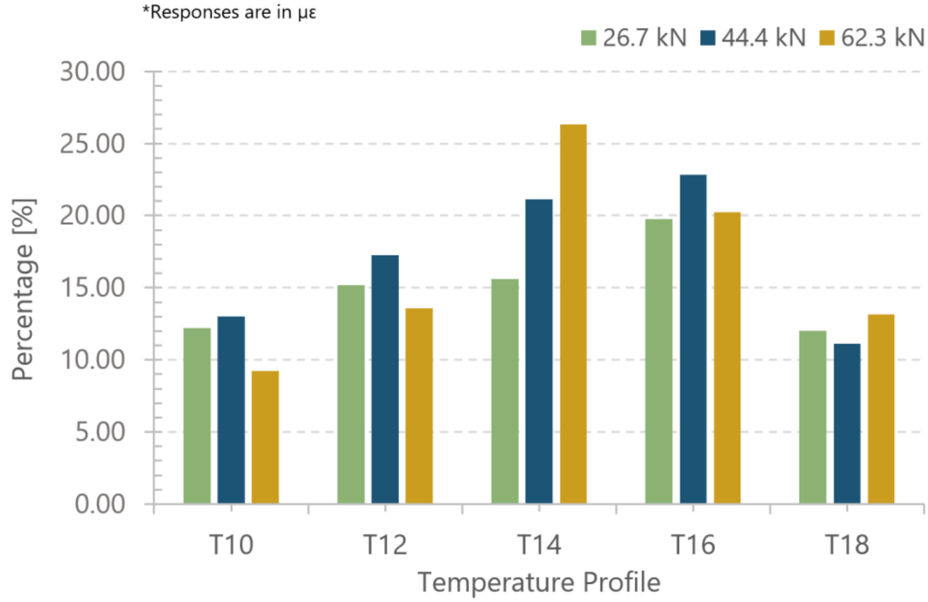

Figure 3-10. Percent difference in maximum tensile strain between LVE and CDVE models

3.3 IMPACT OF LAYER INTERFACE ASSUMPTIONS

Relatively thick AC layers are constructed in lifts. Tack coats are placed between the lifts to ensure proper bonding. Current mechanistic-empirical design and analysis methods are based on the computation of stress, strain, and displacement within the pavement structure. To simplify computations, many assumptions are taken. For instance, all layers are presumed to be fully bonded. Under this assumption, the maximum tensile strain is found at the bottom of the AC layer. Besides, due to high AC thickness, the tensile strain usually has a small magnitude at this location. The assumption of full bonding between layers does not represent the actual field condition. The compaction of each lift does not allow complete bonding between the layers; there is no full aggregate interlock. Previous studies have shown the importance of including an appropriate layer interface in the computation of critical pavement responses.

The layer interface condition has a direct impact on pavement performance. Inadequate lift bonding usually translates into layer slipping and even separation of the layers, causing potholes, cracking, and delamination. In this section, the contribution of interlayer bonding on the top-down cracking is investigated. At high temperatures, the maximum shear stress decreases significantly, increasing the chances of slipping between the AC layers. Due to higher ambient temperatures in Hawaii, interface slippage risk is also higher. Therefore, different constitutive interface models were incorporated to evaluate the impact of interface conditions that may be affecting some of the near surface cracking problems.

The models used assume the AC layer has four lifts with a rough surface interface between them. In this section, an additional case was added, incorporating the Coulomb friction model with maximum shear stress. The highest load (62.3 kN) and temperature profile (T14) were used in this additional case. The maximum shear stress was different at each of the three AC layer interfaces. The values were selected based on the temperature at each lift interface (Romanoschi and Metcalf, 2001).

The maximum tensile strains obtained from the rough interface model were compared to the same responses from the coulomb model. Figures 3.11-a and 3.11-b show the longitudinal tensile strain (e11); along the direction of tire motion and the transverse tensile strain (e33), perpendicular to the direction of motion at the bottom of the AC layer from the fully bonded AC layer model. Figure 3.11-c and 3.11-d show the same responses at the bottom of the last AC lift in the coulomb model. Assuming AC lifts are fully bonded, the maximum e11 and e33 were found at the bottom of the AC -160 $\mu\varepsilon$ in magnitude. When the coulomb-maximum shear model is used, the location of the maximum tensile strain shifted from the bottom of the AC layer to the bottom of the upper AC lift. Moreover, e11 and e33 values increased to 908 and 1136 $\mu\varepsilon$, respectively. At the interface, the elements are in tension. Therefore, no significant effect of confinement on tensile strain is expected at this location.

The results of this section demonstrate the importance of incorporating accurate layer interface condition in the prediction of near-surface distresses.

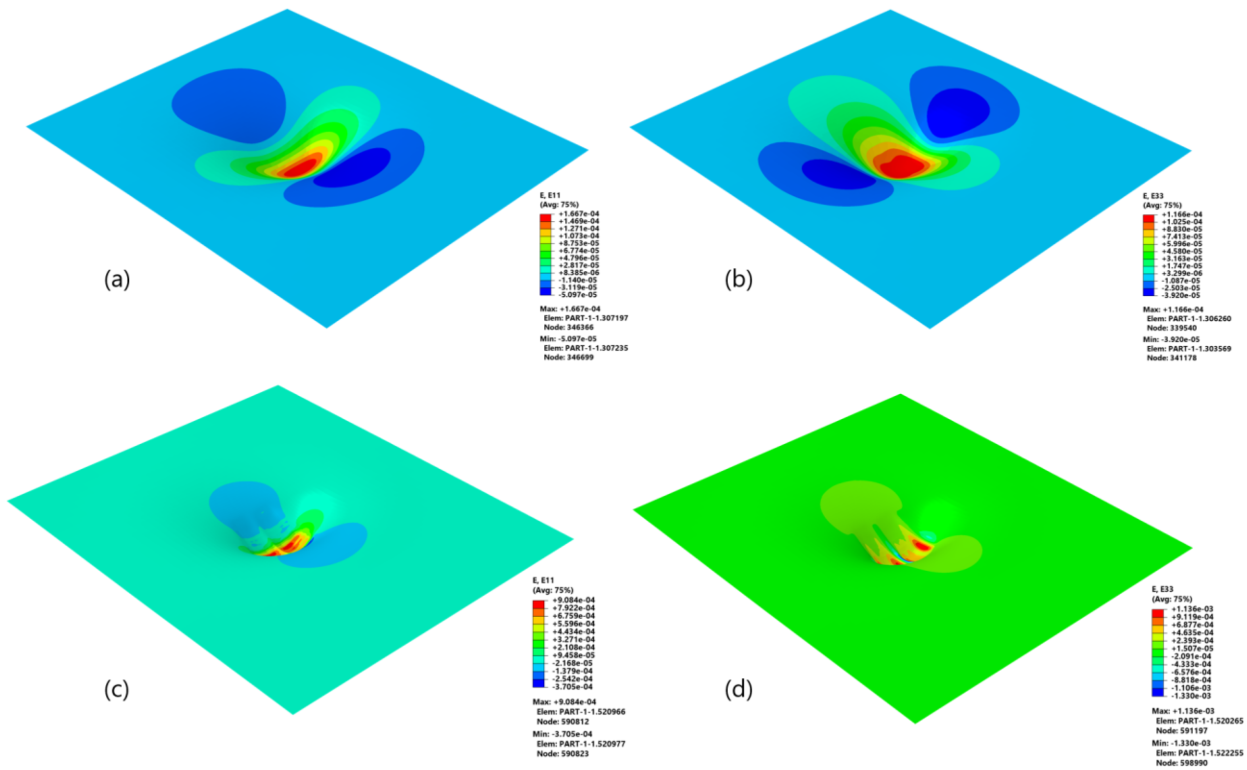

Figure 3-11. (a) longitudinal tensile strain and (b) transverse tensile strain distributions at the bottom of the AC layer – Fully bonded AC lift model. (c) longitudinal tensile strain and (d) transverse tensile strain distributions at the bottom of the top AC lift

CHAPTER 4. CONCLUSIONS AND RECOMMENDATIONS

Near surface pavement responses to traffic loads are among the major factors governing lifetime of many pavements and various preservation treatments. Considering the fact that many of the preservation treatments are thin layer applications on a pavement surface, the importance of capturing near surface pavement responses can be recognized. Some of the factors complicating near surface responses are temperature gradients, non-uniform and 3-D tire contact stresses, material nonlinearities, confinement, and interface conditions. It can be hypothesized that the distresses initiate or concentrates on the surface are the ones that may be affected by confinement more severely.

A numerical modeling approach was used to characterize the effect of those factors using a standard linear viscoelastic and a confined viscoelastic model.

A constitutive model was developed for confinement-dependent linear viscoelastic behavior. The model was then incorporated into finite element pavement models using User-defined MATerial (UMAT). The numerical pavement models were used to quantify the impact of lateral confinement on pavement critical responses under various temperature profiles and tire loadings.

The numerical model includes variables usually omitted from conventional pavement design and analysis, such as dynamic-implicit analysis, continuous moving load with appropriate load amplitude variation, three-dimensional contact stresses, linear viscoelastic, and confinement dependent asphalt concrete behavior, use of infinite elements, coulomb model to represent the layer interface.

The numerical matrix considers two asphalt material models (linear viscoelastic and confinement-dependent viscoelastic), three load levels ranging from low to high, and five temperature profiles.

It is shown with extensive numerical simulations that an accurate representation of near-surface conditions may result in significant differences in pavement responses especially in places like Hawaii. Some of the major findings are as follows:

- The highest compressive confinement is found directly underneath the tire near the tire treads.
- The confinement level increases with increasing temperature.
- The increase in loading causes higher confinement level and deeper zones of influence.
- The effect of confinement depends on relative position of the moving load and therefore time dependent. As tire approaches, move over a point and leaves, the effect of confinement is noticeable.
- Vertical strains in the areas under the tires are significantly affected by confinement. The effect is very sensitive to temperature profile and the reduction in vertical strains with confinement can be as high as 1500 to 2500 microstrains.
- The maximum percent decrease in vertical strain and shear strain due to the incorporation of the CDVE model was found to be 31% and 17.5% for the highest load-temperature combination.

REFERENCES

Archilla, A. R. (2015). Top-down fatigue cracking in high-temperature environments. Transportation Research Record, 2507(1), 128-137.

Archilla, A.R. (2020). Temperature Measurements with Depth and Physical Evidence for the Effect of High Temperature Gradients on Top-Down Fatigue Cracking, Transportation Research Record: Journal of the Transportation Research Board, 2674 (4), pp. 384–396.

Al-Qadi, I. L., Ozer, H., Hernandez, J. and Dhasmana, H. (2018). Mechanistic characterization of thin asphalt overlays for pavement preservation using finite element modeling approach. University of Transportation Center (UTC) Final Report.

Yoo, P., & Al-Qadi, I. (2007). Effect of transient dynamic loading on flexible pavements. Transportation Research Record: Journal of the Transportation Research Board, (1990), 129-140.

Yoo, P. J., Al-Qadi, I. L., Elseifi, M. A., and Janajreh, I. (2006). Flexible pavement responses to different loading amplitudes considering layer interface condition and lateral shear forces. International Journal of Pavement Engineering, 7(1), 73-86.

Al-Qadi, I. L., and Yoo, P. J. (2007). Effect of Surface Tangential Contact Stresses on Flexible Pavement Response (With Discussion). Journal of the Association of Asphalt Paving Technologists, 76.

Al-Qadi, I. L., Elseifi, M. A., Yoo, P. J., Janajreh, I. (2005). Pavement Damage due to Conventional and New Generation of Wide-Base Super Single Tires. Tire Science and Technology, 33(4), 210226.

Corrales-Azofeifa, J.P. and Archilla, A.R. (2018). Dynamic Modulus Model of Hot Mix Asphalt: Statistical Analysis Using Joint Estimation and Mixed Effects, ASCE Journal of Infrastructure Systems, Vol. 24 (3), pp. 04018012-1-12.

Elseifi, M. A., Al-Qadi, I. L., & Yoo, P. J. (2006). Viscoelastic modeling and field validation of flexible pavements. Journal of engineering mechanics, 132(2), 172-178.

Park, S. W., Kim, Y. R., & Schapery, R. A. (1996). A viscoelastic continuum damage model and its application to uniaxial behavior of asphalt concrete. Mechanics of Materials, 24(4), 241-255.

Monismith, C. L., & Secor, K. E. (1962). Viscoelastic behavior of asphalt concrete pavements. In International Conference on the Structural Design of Asphalt PavementsUniversity of

Michigan, Ann Arbor (Vol. 203, No. 1).

Goodrich, J. L. (1988). Asphalt and polymer modified asphalt properties related to the performance of asphalt concrete mixes (with discussion). In Association of Asphalt Paving Technologists Proc (Vol. 57).

Romanoschi, S. A., & Metcalf, J. B. (2001). Characterization of asphalt concrete layer interfaces. Transportation Research Record, 1778(1), 132-139.